ELSEVIER

Desalination 172 (2005) 99–106

DESALINATION

www.elsevier.com/locate/desal

Temporal evolution of resistances in the ultrafiltration of humic substances

Cheng-Fang Lin[a]*, Chung-Hsin Wu[b], Shyue-Wen Kuo[a]

[a]*Graduate Institute of Environmental Engineering, National Taiwan University, Taipei 106, Taiwan*
Tel. +886 (2) 2362-7427; Fax: +886 (2) 2392-7653; email: cflin@ccms.ntu.edu.tw
[b]*Department of Environmental Engineering and Health, Yuanpei University of Science and Technology, Hsinchu, Taiwan*

Received 4 April 2003; accepted 11 June 2004

Abstract

Many ultrafiltration-related studies have emphasized fouling mechanisms, but few works have been done on resistance modeling. This study investigated the temporal variation of different resistances including membrane intrinsic resistance, fouling resistance, and concentration polarization resistance, based on a well established resistance-in-series model. The various resistances were determined at an early stage of ultrafiltration operation. During the initial operation period, the total filtration resistance for ultrafiltration of humic substance solution ranged from 1.9×10^9 to 2.2×10^9 Pa·s/m. The principal resistance of ultrafiltration is from intrinsic membrane resistance, accounting for more than half of the total resistance (56–85%).

Keywords: Ultrafiltration; Humic substances; Fouling; Resistance model

---

1. Introduction

It is well understood that the presence of dissolved organic carbon (DOC) in source water causes a significant flux decline during ultrafiltration (UF) operation. For example, protein fouling is assumed to occur first by blocking pores, and then forming a cake over the blocked areas of the membrane [1,2]. Many resistance models have been developed to elucidate the possible role of various parameters affecting flux decline, including a blocking model for dead-end flow, a mass transfer model and a resistance-in-series model for a cross-flow module [3–8]. The blocking model is primary used for describing the pore blockage phenomenon, but it may not elucidate concentration polarization, gel layer formation and internal adsorption; all these factors contribute to membrane fouling. In the diffusion model, the process of organic compound adsorp-

---

*Corresponding author.

doi:10.1016/j.desal.2004.06.198

tion on a membrane surface is treated as diffusion from a stationary liquid phase to a flat and nonporous surface. The resistance-in-series model describes fouling due to the deposition of organic mass on membrane surfaces (analogous to cake resistance). Three types of resistance — intrinsic membrane, fouling, and gel layer — were considered in series in exerting resistance on water filtration. The accumulation of organic mass with time results in increases in membrane resistance and decreases in permeate flux. Basically, the permeate flux is proportional to pressure gradient and reciprocal of the resistances.

In general, the type of feed as well as its concentration, transmembrane pressure, membrane properties, and flow rate all affect membrane resistances [4,6]. Cho et al. [9] compared three membranes [thin-film composite, polyethersulfone (PES), and sulfonated PES] in terms of their characteristics of flux decline and rejection of natural organic matter (NOM). These membranes exhibited similar flux decline characteristics when filtering a relatively hydrophilic NOM-source water. The thin-film composite membrane, however, has greater NOM rejection than the other membranes when filtering the hydrophilic NOM-source water, while all the membranes have similar NOM rejection with the hydrophobic NOM-source water. Tansel et al. [8] developed a model to characterize the evolution of flux explicitly as a function of time in a cross-flow UF membrane. To correlate flux decline and DOC properties, Cho et al. [10] incorporated specific UV absorbance, water permeability, and mass transfer coefficient into a simple flux decline equation and resistance model.

Many flux decline models were developed using synthetic compounds but not the well characterized, isolated DOC. Since the nature of DOC varies from source to source, it is imperative to investigate various UF resistances with a well characterized DOC. Therefore, in this work a previously developed resistance-in-series model was applied to UF of humic substances. In particular, the temporal evolution of UF resistances in an early operational stage was monitored. The resistances include intrinsic membrane resistance, fouling resistance and gel layer resistance. In this work, the experiments were carried out using a constant feed concentration of humic acid so that the possible biased gel layer resistances obtained using recirculation of concentrated retentate could be avoided.

2. Materials, methods and model

2.1. Materials and methods

The stock humic acid solution was prepared by dissolving 1 g of Aldrich humic acid (sodium salt) in 1 L deionized water (Milli-Q), and filtering through a 0.45-μm membrane filter. The feed solutions (up to 9 mg DOC/L) were supplemented with NaCl to maintain conductivity near 300 μmho/cm and adjusted pH to 7 with 1 N NaOH. The stock humic acid solution and feed solutions were stored at 4°C for subsequent UF experiments.

A single hollow-fiber module (hydrophobic with negatively charged polysulfone; A/G Technology) was used with a length of 29 cm and an area of approximately 9 cm^2. Three types of UF membranes were used, with a nominal molecular weight cutoff (MWC) of 1 kDa, 10 kDa, and 30 kDa. The cross-flow mode was operated in the UF system without recirculating the concentrated stream to avoid changes in feed solution composition. The transmembrane pressure was controlled at three different levels: near 70 kPa (10 psi), 105 kPa (15 psi) and 140 kPa (20 psi). The hollow fiber was initially pre-washed with alcohol for 5 min and then flushed with Milli-Q water for 8 h before the designated experiments. Throughout the experiments (T = 25°C), transmembrane pressure was maintained and permeate flux was monitored. DOC concentration of feed solution for each experiment was quantified in an organic carbon analyzer (QI model 700).

2.2. Model

A resistance-in-series model originated from the hydraulic gradient theorem, which stipulates that the energy loss to maintain a constant fluid velocity is due to the friction on porous media as [4]:

$$J = \frac{T_T}{R_M + R_F + R_G} = \frac{P_T}{R_M + R_F + \Phi P_T} \tag{1}$$

where J is permeate flux (m^3/m^2/s), P_T the transmembrane pressure (Pa), R_M membrane intrinsic resistance (Pa·s/m), R_F fouling resistance (Pa·s/m) due to the interaction between DOC and inner membrane material, and R_G the gel layer/concentration polarization resistance (Pa·s/m). R_G is considered to be proportional to the mass of DOC deposited and the specific resistance of the gel layer. As the gel layer is compressed, the resistance tends to increase with applied pressure [11]. Therefore, R_G is expressed as a function of transmembrane pressure with $R_G = \Phi P_T$, where Φ is dependent on the specific membrane system and can be determined from experimental data [6].

2.3. Determination of P_T, R_M, R_F, and Φ

The transmembrane pressure is calculated by Eq. (2):

$$P_T = \frac{P_i + P_o}{2} - P_p \tag{2}$$

where P_i, P_o, and P_p are UF inlet, outlet, and atmospheric pressure, respectively. The R_M is determined in a deionized water UF system with a fresh hollow-fiber module as:

$$J = \frac{P_T}{R_M} \tag{3}$$

By varying transmembrane pressure and plotting $(1/J)$ vs. $(1/P_T)$, the slope of the straight line yields the R_M. To determine R_F and Φ, the flux as a function of transmembrane pressure and feed DOC concentration was monitored. The plots of $(1/J)_t$ vs. $(1/P_T)$ were constructed, and the slope and the intercept yield $R_M + R_F$ and Φ, respectively.

$$\left(\frac{1}{J}\right)_t = \Phi + \frac{R_M + R_F}{P_T} \tag{4}$$

R_F is then obtained by subtracting the R_M value [Eq. (3)] from $R_M + R_F$ [Eq. (4)], and R_G is equal to Φ times P_T. It is important to note that the resistances are dynamic variables except for the intrinsic membrane resistance. They are continuously changing until a particular UF system reaches the equilibrium state.

3. Results and discussion

Table 1 lists the permeate flux of the UF experiments under various humic acid concentrations, transmembrane pressures and membrane sizes. The UF permeate flux depends largely on membrane MWC and transmembrane pressure. For example, the system with a 1 kDa membrane at DOC = 4 mg/L solution exhibits a permeate flux of about 8×10^{-6} m^3/m^2/s at 70 kPa (P10); it increases to 13×10^{-6} m^3/m^2/s at 140 kPa (P20). As the MWC increases from 1 kDa to 30 kDa, the permeate fluxes significantly increase to 48×10^{-6} m^3/m^2/s at 70 kPa and 80×10^{-6} m^3/m^2/s at 140 kPa.

The effect of DOC concentration on UF permeate flux can also be seen in Table 1. It appears that the initial fluxes of UF membrane at

Table 1
Permeate flux of UF systems at 10^{-6} $m^3/m^2/s$

DOC, mg/L	1 kDa			10 kDa			30 kDa		
	P10	P15	P20	P10	P15	P20	P10	P15	P20
2:									
Initial flux				31.2	49.3	62.4			
24-h flux				24.7 (79)	32.6 (66)	39.1 (63)			
4:									
Initial flux	7.5	10.5	13.3	34.4	52.1	59.6	47.5	62.4	79.6
24-h flux	6.9 (91)	8.4 (80)	11.4 (86)	24.2 (70)	32.6 (63)	37.2 (63)	30.5 (64)	39.1 (63)	46.5 (58)
9:									
Initial flux				28.4	44.2	58.6			
24-hr flux				20.7 (73)	30.7 (69)	39.1 (67)			

Notes: P10, P15 and P20 represent transmembrane pressure 70 kPa, 105 kPa, and 140 kPa, respectively.
Numbers in parentheses represent the percentage of the initial flux.

the same transmembrane pressure with three different DOC concentrations are quite close (e.g., 59–62×10^{-6} $m^3/m^2/s$ at 140 kPa), indicating an insignificant role of DOC concentration on permeate flux. This may indicate a pore plugging phenomenon. It was further noted that the flux decline of the three DOC concentrations was similar to other UF systems after 24 h (e.g., 63–69% of the initial flux at 105 kPa). However, the finding of the insignificant role of the feed DOC concentration on flux decline may not be applicable to other systems with higher DOC concentrations, or after a prolonged period of UF operation.

The R_M values as a function of transmembrane pressure were determined by using Eq. (3), and the values obtained are 9.5×10^9, 2.0×10^9 and 1.4×10^9 Pa·s/m for 1, 10, and 30 kDa, respectively. Since operating conditions as well as the type of membrane used are different among studies, the comparison of these intrinsic resistance values must be made with care. Nonetheless, these values are close to the literature numbers, e.g., 1–2×10^9 Pa·s/m for a polysulfone membrane with 30 kDa [12].

As stated previously, the permeate flux of a specific system was measured as a function of time at three different transmembrane pressures. The reciprocal plots of permeate fluxes vs. transmembrane pressures yield a good correlation (R^2>0.97) for those data at t<660 min. Consequently, the subsequent discussion is limited to UF operation up to t = 660 min, representing the evolution of membrane resistance in an earlier UF operational stage. Fig. 1 shows the time evolution of Φ values as a function of membrane size (Fig. 1a) and feed DOC concentration (Fig. 1b). Clearly, the Φ values, representing the resistance due to concentration polarization and gel layer, increase with time. As would be expected, the highest Φ value (8.6×10^3 s/m) after 660 min is associated with the smallest membrane size (1 kDa).

The effect of DOC concentration on Φ can be envisioned as three stages corresponding to a fast interaction, slow association and equilibrium state. The near pseudo-"maximum" state is reached in about 200 min in most cases. Indeed, the time-dependent Φ profiles are similar to adsorption isotherms; typically a "plateau" is

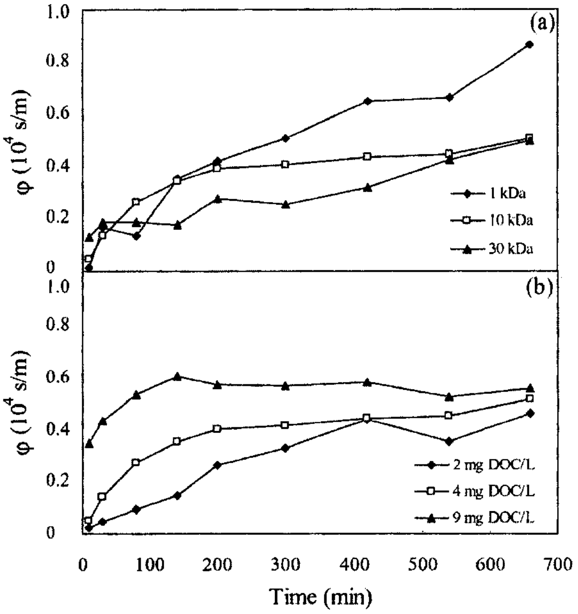

Fig. 1. Evolution of Φ as a function of time in UF systems. (a) 4 mg DOC/L humic acid; (b) 10 kDa membrane.

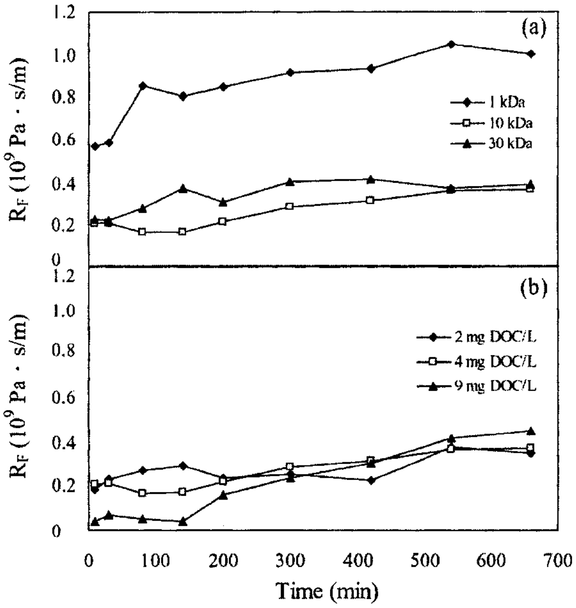

Fig. 2. Fouling resistance (R_F) as a function of time in UF systems. (a) 4 mg DOC/L humic acid; (b) 10 kDa membrane.

reached, indicating a maximum or saturation capacity of membrane for DOC. The build-up of concentration polarization and gel layer is analogous to the formation of a sorption layer on the inner membrane surface.

For comparison, the Φ values from related studies range from 2.2×10^4 to 3.5×10^5 s/m [4,6, 12]. The reason for the smaller Φ numbers observed in the present study is, among others (e.g., experimental conditions), mainly due to the earlier stage of UF operation (up to 660 min). Yeh and Wu [6] have expressed Φ as a function of fluid tangential velocity (to the power of −0.77) and the feed (polyvinylpyrrolidone) concentration (to the power of 0.3). The gel-layer-related R_G can be further classified into reversible and semi-reversible polarized layers [12].

The temporal changes of R_F as a function of membrane MWC and DOC concentration are presented in Fig. 2a and 2b, respectively. The R_F values increase with time and reache a plateau state quickly, indicating a fast build-up of foulant. The development of R_F with time is more evident for a membrane with a smaller pore size (1 kDa), albeit with little variation. For example, R_F ranges from 5.7×10^8 to 1×10^9 and 2.3×10^8 to 3.9×10^8 Pa·s/m, for 1 kDa and 30 kDa membrane systems, respectively. It is noted that DOC concentration plays an insignificant role on R_F (Fig. 2b); at t = 660 min, the R_F value is similar for all three concentrations. This is understandable as the reaction of foulants with the membrane surface is limited to the surface-reacting sites. Once the sites are saturated with foulants resulting in pore blocking, R_F becomes a constant value, regardless of the feed solute concentration.

The ratios of R_F/R_M are 29, 20 and 11% for 30, 10, and 1 kDa, respectively, at t = 660 min (Fig. 3). Clearly, the ratio is higher for a loose membrane than that for a tight one. Table 2 summarizes the proportions of various resistances in the UF systems based the flux data up to t =

Table 2
Total resistance (10^9 Pa·s/m) and distribution (%) of various resistances in UF systems

DOC, mg/L	R_M, %			R_F, %			R_G %			Total resistance, 10^9 Pa·s/m		
	P10	P15	P20	P10	P15	P20	P10	P15	P20	P10	P15	P20
4:												
1 kDa	85	83	82	9	9	8	6	8	10	10.7	11.5	12.2
10 kDa	71	68	65	15	13	12	14	19	23	2.5	2.8	3.1
30 kDa	62	59	56	20	17	16	18	24	28	1.9	2.2	2.5
2:												
10 kDa	75	71	67	13	12	12	12	17	21	2.7	2.8	3.0
9:												
10 kDa	72	66	61	15	15	14	13	19	25	3.0	3.1	3.1

P10, P10 and P20 represent transmembrane pressures 70 kPa, 105 kPa, and 140 kPa, respectively.

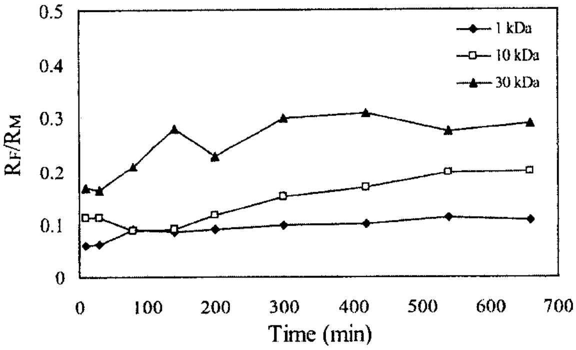

Fig. 3. R_F/R_M as function of a time in the UF system with 4 mg DOC/L humic acid.

660 min. Clearly, the principal resistance during filtration is from R_M, accounting for more than half of the total resistance (56–85%). The variation in different resistances is mainly due to the difference in membrane size and, to a lesser extent, pressure; concentration exerts the least impact. For example, the percentage of various resistances for the 10 kDa membrane with three different DOC concentrations is comparable (e.g., 71–75% for R_M and 13–15% for R_F at 70 kPa). A loose membrane (30 kDa) is more vulnerable to the accumulation of foulants and gel layer formation than the tight membrane. For instance, when comparing the resistance at the same DOC concentration (4 mg/L) and transmembrane pressure (P15, 105 kPa), the R_F value increased from 9% for the 1 kDa membrane to 17% for the 30 kDa fiber. The exact reasons(s) is unclear; perhaps, the DOC is more likely to penetrate into the inner pores, and the resultant deposit/associate at the deeper layers may be responsible for a higher resistance.

The temporal evolution of UF membrane resistance determined in this study is limited to a narrow time frame. Thus, it may explain that our finding — R_M is the principal resistance — is not comparable with those reported by others [4,12, 13]. For example, Jiraratananon and Chanachai [12], in a study of passion fruit juice, indicated that UF (polysulfone with 30 kDa) resistance was most due to polarized gel layer (49–84%) at temperatures of 30 to 40°C, and due to a foulant layer (56–62%) at a higher temperature (50°C). Nonetheless, Fan et al. [14] reported that the irreversible resistance caused by NOM in a microfiltration membrane accounted for only 4–11% of the total resistance. Although the flux data monitored in this work are approximately 60% of the initial values, which are far below those (say 5%) reported by others, the results do provide valuable information about the evolution of UF resistance in an early stage of UF operation. After all, these resistances eventually determine the latter stage of UF operation with respect to flux and membrane fouling.

4. Conclusions

The total filtration resistance during the initial stage for UF humic substance solution ranges from 1.9×10^9 to 12.2×10^9 Pa·s/m under the present experimental conditions. The intrinsic membrane resistances of 1 kDa, 10 kDa, and 30 kDa polysulfone membranes were determined to be 9.5×10^9, 2.0×10^9, and 1.4×10^9 Pa·s/m, respectively, based on the resistance-in-series model. The resistance is mainly dependent on the membrane MWC size used and, to a lesser extent, operating transmembrane pressure the concentration of the feed solution. The principal UF resistance during the initial operating stage is from intrinsic membrane resistance, accounting for more than half of the total resistance (56–85%). Again, the variation is primarily due to the difference in membrane size.

Acknowledgement

The authors would like to thank the National Science Council of the Republic of China for financially supporting this research under Contract No. NSC 89-2211-E-002-078.

References

[1] C.C. Ho and A.L. Zydney, J. Membr. Sci., 209 (2002) 363–377.

[2] C.C. Ho and A.L. Zydney, Ind. Engng. Chem. Res., 40 (2001) 1412–1421.

[3] M.M. Clark and P. Lucas, J. Membr. Sci., 143 (1998) 13–25.

[4] B.H. Chiang and M. Cheryan, J. Food Sci., 51 (1986) 340–344.

[5] W.R. Bowen, J.I. Calvo and A. Hernandez, J. Membr. Sci., 101 (1995) 153–165.

[6] H.M. Yeh and H.H. Wu, J. Membr. Sci., 124 (1997) 93–105.

[7] H.M. Yeh, T.W. Cheng and H.H. Wu, Sep. Purif. Technol., 13 (1998) 171–180.

[8] B. Tansel, W.Y. Bao and I.N.Tansel, Desalination, 129 (2000) 7–14.

[9] J. Cho, G. Amy and J. Pellegrino, Desalination, 127 (2000) 283–298.

[10] J. Cho, G. Amy, Y. Yoon and J. Sohn, Desalination, 142 (2002) 245–255.

[11] A.A. McCarthy, P.K. Walsh and G. Foley, J. Membr. Sci., 201 (2002) 31–45.

[12] R. Jiraratananon and A. Chanachai, J. Membr. Sci., 111 (1996) 39–48.

[13] K.H. Choo and C.H. Lee, Water Res., 30 (1996) 1771–1780.

[14] L. Fan, J.L. Harris, F.A. Roddick and N.A Booker, Water Res., 35 (2001) 4455–4463.